

# N-Myc Downstream-Regulated Gene 2 (NdrG2) Is Involved in Ischemia–Hypoxia-Induced Astrocyte Apoptosis: a Novel Target for Stroke Therapy

Yu-Long Ma<sup>1</sup> · Li-xia Zhang<sup>2</sup> · Guang-lin Liu<sup>1</sup> · Yanhong Fan<sup>3</sup> · Ye Peng<sup>4</sup> · Wu-Gang Hou<sup>1</sup>

Received: 21 August 2015 / Accepted: 23 February 2016 / Published online: 6 May 2016  
© Springer Science+Business Media New York 2016

**Abstract** Nearly all clinical trials that have attempted to develop effective strategies against ischemic stroke have failed, excluding those for thrombolysis, and most of these trials focused only on preventing neuronal loss. However, astrocytes have gradually become a target for neuroprotection in stroke. In previous studies, we showed that the newly identified molecular N-myc downstream-regulated gene 2 (NdrG2) is specifically expressed in astrocytes in the brain and involved in some neurodegenerative diseases. However, the role of NDRG2 in ischemic stroke remained unclear. In this study, we investigated the role of NDRG2 in middle cerebral artery occlusion (MCAO)-induced focal cerebral ischemia and in oxygen–glucose deprivation (OGD)-induced cellular apoptosis in the M1800 astrocyte cell line. NDRG2 mRNA and protein expression began to increase at 6 and 2 h after

reperfusion and peaked at 24 h in the ischemic penumbra and in M1800 cells, as detected by RT-PCR and Western blotting. Double immunofluorescence staining showed that the number of apoptotic cells increased as the NDRG2-positive signal increased and that the NDRG2 signal was sometimes co-localized with TUNEL-positive cells and translocated from the cytoplasm to the nucleus in both the ischemic penumbra and the M1800 cells. Using a lentivirus, we successfully constructed two stable astrocytic cell lines in which NDRG2 expression was significantly up- or down-regulated. NDRG2 silencing had a proliferative effect and reduced the percentage of apoptotic cells, reactive oxygen species (ROS) production, and cleaved Caspase-3 protein expression following OGD, whereas NDRG2 over-expression had the opposite effects. In conclusion, NDRG2 is involved in astrocyte apoptosis following ischemic–hypoxic injury, and inhibiting NDRG2 expression significantly reduces ROS production and astrocyte apoptosis. These findings provide insight into the role of NDRG2 in ischemic–hypoxic injury and provide potential targets for future clinical therapies for stroke.

Yu-Long Ma, Li-xia Zhang and Guang-lin Liu contributed equally to this work.

**Electronic supplementary material** The online version of this article (doi:10.1007/s12035-016-9814-5) contains supplementary material, which is available to authorized users.

✉ Ye Peng  
pengye1985@163.com

✉ Wu-Gang Hou  
gangwuhou@163.com

<sup>1</sup> Department of Anesthesiology, Xijing Hospital, The Fourth Military Medical University, Xi'an 710032, China

<sup>2</sup> First Affiliated Hospital to Chinese PLA General Hospital, Beijing 100048, China

<sup>3</sup> Department of Cardiology, Xijing Hospital, The Fourth Military Medical University, Xi'an 710032, China

<sup>4</sup> Department of Orthopaedics, Air Force General Hospital of PLA, Beijing 100142, China

**Keywords** NdrG2 · Astrocyte · Apoptosis · MCAO · OGD · Neuroprotection

## Abbreviations

NdrG2	N-Myc downstream-regulated gene 2
MCAO	Middle cerebral artery occlusion
OGD	Oxygen–glucose deprivation
CNS	Central nervous system
GFAP	Glial fibrillary acidic protein
ROS	Reactive oxygen species

## Introduction

Over the past two decades, over 1000 clinical trials of stroke treatments have failed to demonstrate a benefit, with the exception of thrombolytics [1]. Although many targets have been pursued, including antioxidants, calcium channel blockers, glutamate receptor blockers, and neurotrophic factors, the focus has often been on the mechanisms of neuronal injury because neurons are more vulnerable to the detrimental effects of ischemia due to the loss of energy and nutrition. In fact, both energy and nutritional resources are transported by astrocytes, which are the most abundant cell type in the brain and play key roles in the physiology and pathology of the central nervous system (CNS) [2]. Astrocytes perform various functions including the mediation of synaptic transmission through removal of the majority of glutamate from the synaptic cleft, balance of ions and fluid in the extracellular space, formation of the blood–brain barrier, control of energy metabolism, and regulation of blood flow through contact with the brain vasculature [3–5]. Therefore, astrocyte dysfunction is now considered one of the key factors in neuron death after ischemic stroke [6]. Previous studies show that astrocyte apoptosis, which seriously impairs astrocyte functions, contributes largely to ischemia stroke-induced neuronal injury [7]. Thus, the investigation of astrocyte-specific molecular mechanisms to inhibit astrocyte apoptosis might provide novel targets for the development of neuroprotective strategies for ischemic stroke.

N-Myc downstream-regulated gene 2 (NDRG2) was first identified in a normal human brain cDNA library in 2001 [8] and was subsequently found to be highly expressed in the rat brain [9]. In a recent study, we demonstrated that NDRG2 was primarily expressed in astrocytes in the mouse brain [10]. Another recent study showed that NDRG2-positive astrocytes were more abundant and more evenly distributed in the brain than glial fibrillary acidic protein (GFAP)-positive astrocytes [11], which is a classic astrocyte marker. Thus, NDRG2 is considered a new marker for astrocytes. However, the function of NDRG2 in astrocytes remains unclear.

Several studies have shown that NDRG2 is related to several important functions and pathophysiological processes in the CNS. Mitchelmore et al. [12] observed that both the RNA and protein expression levels of NDRG2 were up-regulated in patients with Alzheimer's disease (AD). Takahashi et al. [13] reported down-regulation of NDRG2 expression in the rat frontal cortex after long-term antidepressant administration and repeated electroconvulsive treatment. Furthermore, increased NDRG2 protein expression is found in the hippocampus of chronically stressed rats [14], and NDRG2 is also associated with frontotemporal lobar degeneration [15]. Our previous study was the first to report the spatial–temporal expression of NDRG2 in the rat brain after transient focal cerebral ischemia [16] and indicated that NDRG2 in

astrocytes is involved in the development of the pathological processes of cerebral ischemia. However, the mechanisms that underlie the effects of NDRG2 in cerebral ischemic injury remain to be elucidated, and NDRG2 may become a new molecular target for the treatment of ischemic stroke.

## Materials and Methods

### Animals

Forty 6-month-old male C57BL/6 mice (23–25 g) were obtained from the Laboratory Animal Center of the Fourth Military Medical University. These mice were randomly assigned to one of the following five groups ( $n=8$  in each group): the sham-operated group or the 2-, 6-, 12-, or 24-h ischemia/reperfusion (I/R) group. The mice in the sham group received the same surgery, but middle cerebral artery occlusion (MCAO) was not performed. The mice in the I/R groups were subjected to 60-min MCAO and were then killed at 2, 6, 12, and 24 h after reperfusion. All animal experimental procedures followed a protocol approved by the Ethics Committee for Animal Experimentation of the Fourth Military Medical University, China.

### MCAO

MCAO was performed as previously described [17]. Cerebral blood flow was monitored using laser Doppler flowmetry (PeriFlux 5000; Perimed AB, Järfälla, Sweden). During surgery, occlusion was considered successful when blood flow declined to less than 15 % of the pre-ischemic baseline level; otherwise, the animals were discarded. Following 1 h of transient occlusion, cerebral blood flow was restored by removing the nylon suture for 2, 6, 12, and 24 h. Physiological parameters, such as blood pressure and blood gas, were monitored.

### Immunofluorescence Double-Labeling

Paraffin sections were deparaffinized in xylene and rehydrated. The sections were incubated with proteinase K (10  $\mu\text{g}/\text{mL}$ ) for 15 min at 37 °C for antigen retrieval, and nonspecific antibody-binding sites were blocked with 1 % BSA–PBS. The sections were incubated with an anti-NDRG2 rabbit monoclonal antibody (1:100; Cell Signaling Technology, USA) and an anti-GFAP mouse monoclonal antibody (1:400; Cell Signaling Technology) in 1 % BSA–PBS overnight at 4 °C. The sections were then washed in TBS and incubated with an anti-mouse fluorescein isothiocyanate (FITC)-tagged secondary antibody (1:200; CWBIO, Peking, China) and an anti-rabbit CY3-tagged secondary antibody (1:200; CWBIO, Peking, China) for 2 h at room temperature. 4',6-Diamidino-2-phenylindole (DAPI) (1 ng/ $\mu\text{L}$ ) was used to

stain the nuclei. The sections were mounted with 50 % glycerol and examined under a fluorescence microscope.

### Cell Culture

MA1800-57 cells were purchased from Scienecell and cultured at 37 °C in conditions of 5 % CO<sub>2</sub> and 95 % oxygen in Dulbecco's modified Eagle's medium (DMEM) supplemented with 10 % fetal bovine serum, streptomycin (100 µg/ml), and penicillin (100 units/mL). The cells were divided into five groups: (1) the Con group: cells without lentiviral infection; (2) the KD-NC group: cells infected with a negative control lentivirus; (3) the KD group: cells infected with a lentivirus that knocked down NDRG2 expression; (4) the OE-NC group: cells infected with a negative control lentivirus (LEN-Lacz); and (5) the OE group: cells infected with a lentivirus that up-regulated NDRG2 expression (LEN-NDRG2).

### Construction of a Stable Cell Line with Down-regulated NDRG2 Expression

The lentivirus that could disrupt NDRG2 expression was purchased from Genepharma Company (Shanghai, China). The NDRG2-targeting sequence was 5'-GGGATATGCAAGAGATCATAC-3', and the negative control sequence was 5'-TTCTCCGAACGTGTCACGT-3'. The lentivirus contained a green fluorescent protein (GFP) reporter gene, which resulted in stable green fluorescence in transfected cells. Briefly, 450 µl of cell culture medium and 50 µl of lentivirus were added to M1800 cells in 24-well plates. After 48–72 h, we observed that 70–80 % of the cells expressed GFP, as detected by fluorescence microscopy (Olympus, Tokyo, Japan; Supplemental Fig. 1), verifying successful lentiviral transfection. Then, we cultured the transfected cells for proliferation and screened them for green fluorescence using flow cytometry. Western blotting confirmed that the cell line exhibited stable down-regulation of NDRG2 expression (Supplemental Fig. 2).

### Construction of a Stable Cell Line with Up-regulated NDRG2 Expression

To produce the lentivirus, 293T cells were co-transfected with pLEN-NDRG2 or pLEN-Lacz. The plasmids were amplified in *E. coli* DH5 cells, purified using a Plasmid Maxi Kit (Qiagen, Valencia, CA, USA), and transfected into 70 % confluent 293T cells using Lipofectamine 2000 (Invitrogen). Lentiviral particles were harvested from the supernatant 72 h after the transfection and purified by ultracentrifugation. These particles are hereafter referred to as LEN-NDRG2 and LEN-Lacz (negative control). Stably infected M1800 cells were selected using blasticidin (10 µg/ml; Sigma, USA),

which killed the uninfected cells. Western blotting confirmed that the LEN-NDRG2-infected M1800 cells stably over-expressed NDRG2 (Supplemental Fig. 2).

### EdU Proliferation Assay

The proliferative capacity of the different groups of cells was determined using the Click-iT EdU (5-ethynyl-20-deoxyuridine) Alexa Fluor 594 Imaging Kit (Invitrogen, USA) according to the manufacturer's protocol. Briefly, cells that were cultured in 96-well plates were incubated with 10 µM EdU for 3 h before they were fixed, permeabilized, and stained with EdU. Cell nuclei were stained with DAPI (1 ng/µl) for 10 min. EdU is a nucleoside analog of thymidine that is only incorporated into DNA during active DNA synthesis in proliferating cells. After EdU was incorporated into the cells, a fluorescent molecule was added that reacted specifically with EdU, enabling fluorescent visualization of proliferating cells. The percentage of EdU-positive cells was calculated from five random fields in three wells.

### Cell Cycle Analysis

The cell cycle was assessed by flow cytometry. The cells of different groups were collected by trypsinization and centrifuged twice in PBS. The cells were then fixed in pre-cooled 70 % ethanol at –20 °C and stained with propidium iodide (PI) solution. The DNA content was determined by flow cytometry using CellQuest Software. For each sample, 10,000 events were counted (FACSCalibur, Becton–Dickinson, USA). The percentage of cells that were in a particular cell cycle stage was calculated using ModFit software (Becton–Dickinson, USA).

### Oxygen and Glucose Deprivation and Reperfusion

The cells of different groups were washed twice in DMEM without glucose (oxygen and glucose deprivation (OGD) medium) and transferred to DMEM without glucose. Then, the cells were transferred to a modular incubator chamber. The chamber was flushed with a 95 % N<sub>2</sub>/5 % CO<sub>2</sub> gas mixture at 3 L/min for 30 min at room temperature. The chamber was then sealed and placed in a 37 °C container. OGD was carried out for 4 h. Following OGD, the cells were incubated in DMEM with glucose (without fetal bovine serum) for an additional 2, 6, 12, and 24 h of reperfusion under normal conditions and then collected for subsequent analysis.

### RT-PCR

For reverse transcription RT-PCR, 50 mg of tissue ( $n=5$  in each group) and cells with different reperfusion times (2, 6, 12, and 24 h as well as sham) were collected

immediately. Total RNA was isolated from each sample using TRIzol reagent (Invitrogen, Carlsbad, CA, USA) and then quantified. Two micrograms of total RNA was reverse-transcribed using reverse transcriptase (Promega, Madison, WI, USA) according to the manufacturer's instructions. All PCR experiments were performed using Taq polymerase (Promega) with the following primers: *ndrg2* sense (5'-CAGAACTTCGTGCGGGTTCA-3'), *ndrg2* antisense (5'-GAATGTAGGCTCCGGCTCCA-3'), GAPDH sense (5'-CATCCGTAAAGACCTCTATGCCAAC-3'), and GAPDH antisense (5'-ATGGAGCCACCGATCCACA-3'). The PCR products were resolved on a 1 % agarose gel containing ethidium bromide, and the bands were visualized using ultraviolet light.

### Measurement of Reactive Oxygen Species

After exposed to oxygen and glucose deprivation and reperfusion (OGD-R), different groups of cells were washed with PBS and loaded with DCFH-DA (5  $\mu$ M) from Reactive Oxygen Species Assay Kit (Beyotime Institute of Biotechnology, Jiangsu, China) for 40 min. After a further wash with PBS, cell suspensions were collected into a 96-well flat bottom black plate to determine the relative fluorescent intensity (RFI,  $\lambda_{ex}$  485 nm,  $\lambda_{em}$  535 nm) by Tecan GENios fluorescence microplate reader. The DMEM medium was used as blank. The RFI over control was calculated as the measured reactive oxygen species (ROS) production levels.

### Cell Fraction Assay

Twenty-four hours after the cells were exposed to OGD, nuclear extracts were prepared in accordance with the protocol of the NE-PER Nuclear and Cytoplasmic Extraction Reagents Kit (Pierce, Rockford, IL, USA). Briefly, M1800 cells were washed twice with ice-cold PBS, and 200 ml of ice-cold cytoplasmic extraction reagent I was added. The cells were incubated on ice for 10 min, and then 11 ml of ice-cold cytoplasmic extraction reagent II was added. The cells were incubated on ice for 1 min, and the tube was then centrifuged for 5 min at maximum speed in a microcentrifuge (16,000  $\times$  g). The supernatant fraction (cytoplasmic extract) was immediately transferred to a clean pre-chilled tube, and 100 ml of ice-cold nuclear extraction reagent was added to the insoluble fraction by vortexing for 15 s every 10 min for a total of 40 min. The tube was centrifuged at maximum speed in a microcentrifuge for 10 min. The nuclear extract fraction was then moved to a clean pre-chilled tube. All extracts were analyzed by Western blotting.

### Western Blot Analysis

For Western blot analysis, 50 mg of tissues ( $n=5$  in each group) and cells with different reperfusion times (sham and 2, 6, 12, and 24 h) were lysed in modified radioimmunoprecipitation assay buffer. The protein concentration was measured using the bicinchoninic acid (BCA) protein assay (Pierce, Rockford, IL, USA). Proteins were separated by sodium dodecyl sulfate polyacrylamide gel electrophoresis (SDS-PAGE) and transferred to Hybond ECL nitrocellulose membranes (Amersham Biosciences, Little Chalfont, Buckinghamshire, UK). Mouse anti-NDRG2 (1:1000; Cell Signaling Technology), rabbit anti-cleaved Caspase-3 (1:1000; Cell Signaling Technology), rabbit anti-Caspase-3 (1:1000; Cell Signaling), rabbit anti-Histone H2A.X (1:300; Signalway Antibody, USA), mouse anti- $\beta$ -actin (1:1000; Cell Signaling), and mouse anti-GAPDH antibodies (1:1000; Cell Signaling) were used for immunoblotting. The membranes were then incubated with an HRP-conjugated secondary antibody for 2 h. Protein bands were visualized using the LI-COR Odyssey System (LI-COR Biotechnology, USA).

### Flow Cytometric Analysis

After OGD and 24 h of reperfusion, cell apoptosis was assayed by flow cytometry. Briefly, the cells of different groups were washed with  $1\times$  annexin V-FITC binding buffer prior to being stained with annexin V-FITC and PI for 15 min at room temperature in the dark. The stained cells were immediately analyzed using flow cytometry. Apoptotic and necrotic cells were quantified by annexin V binding and PI uptake, respectively. The annexin V-FITC+/PI- cell populations were considered to represent apoptotic cells.

### TUNEL and NDRG2 Immunofluorescence Double-Labeling

Apoptosis was quantified using a commercially available fluorescent terminal deoxynucleotidyl transferase nick-end labeling (TUNEL) kit in accordance with the manufacturer's protocol (Roche Diagnostics Corporation, USA). Coronal brain sections from mice that were subjected to MCAO and coverslips with M1800 cells that were exposed to OGD-R were incubated with a rabbit anti-NDRG2 antibody (1:100; Cell Signaling) and an anti-rabbit CY3-tagged secondary antibody and then stained with DAPI (1 ng/ $\mu$ L). The sections were mounted with 50 % glycerol and examined under a fluorescence microscope.

### Statistical Analysis

The data are presented as the mean  $\pm$  S.D. Differences among the groups were analyzed using one-way ANOVA.

Differences between two groups were analyzed using a two-tailed Student's *t* test with SPSS 13. A *p* value <0.05 was considered statistically significant.

## Results

### Temporal Expression of NDRG2 in the Ischemic Penumbra

Compared to the expression in the sham-operated group, in the ischemia–reperfusion (I/R) groups, NDRG2 mRNA (Fig. 1a) and protein (Fig. 1b) expression in the ischemic penumbra began to significantly increase at 6 h after reperfusion and peaked at 24 h (\**p*<0.05; Fig. 1c).

We detected NDRG2 expression in different parts of the ischemic penumbra (cortex, striatum, hippocampus) at 24 h after reperfusion. Compared to the expression in the sham-operated group, in the I/R groups, NDRG2 protein expression in the cortex and striatum of the ischemic penumbra significantly increased at 24 h after reperfusion (\**p*<0.05; Fig. 2),

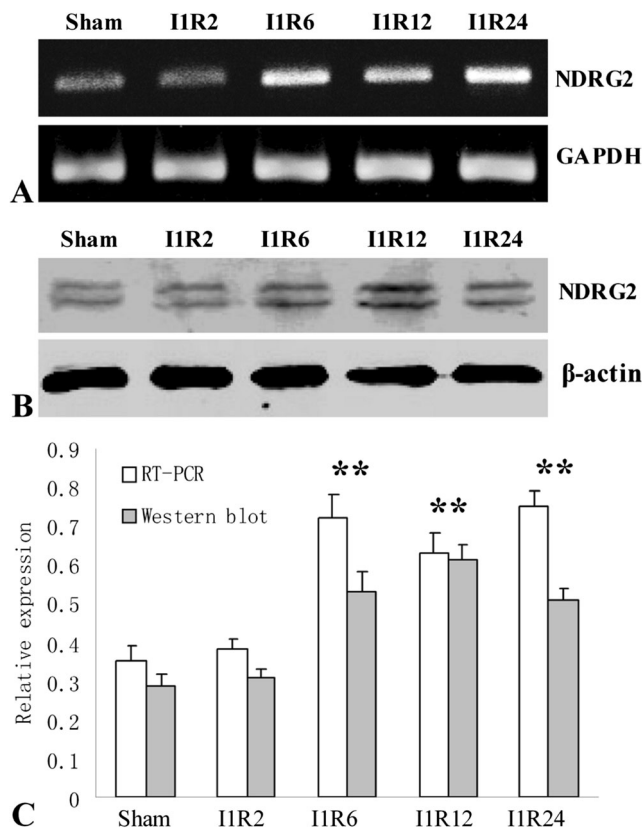


**Fig. 1** Temporal expression of NDRG2 in the ischemic penumbra, as demonstrated by RT-PCR and Western blot analysis. **a** NDRG2 mRNA level and **b** protein expression in the ischemic penumbra at 2, 6, 12, and 24 h after reperfusion and in the sham-operated group. **c** The relative density of NDRG2 protein expression versus  $\beta$ -actin protein expression was plotted. The data are expressed as the mean  $\pm$  S.D. *t* Test: \**p*<0.05 vs. the sham group

while NDRG2 protein expression in the hippocampus of the ischemic penumbra has no significant difference compared to the sham-operated group (Fig. 2).

### Location and Expression of NDRG2 in the Ischemic Penumbra

NDRG2 protein (red) was co-localized with GFAP protein (green) in both the sham-operated and ischemic brains, consistent with an astrocytic localization. NDRG2 expression in the ischemic penumbra at 24 h after reperfusion was higher than the expression in the sham-operated group (Fig. 3). Furthermore, NDRG2 protein expression was weak in the nucleus and strong in the cytoplasm in the sham-operated group (Fig. 4). However, the NDRG2 protein expression was strong in the nucleus and the NDRG2 protein (red) was co-localized with DAPI staining (blue) in the ischemic penumbra at 24 h after reperfusion.

### Cellular NDRG2 Co-localization with Apoptotic Cells

TUNEL staining showed that few apoptotic cells were present in the sham hemisphere, whereas the number of apoptotic cells in the ischemic penumbra was significantly increased at 24 h after reperfusion (Fig. 5). Furthermore, double immunofluorescence for TUNEL and NDRG2 demonstrated that some of the TUNEL-positive cells were co-localized with NDRG2-positive cells in the ischemic penumbra following I/R.

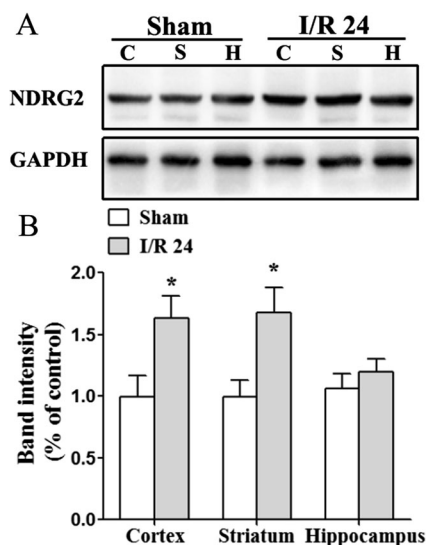
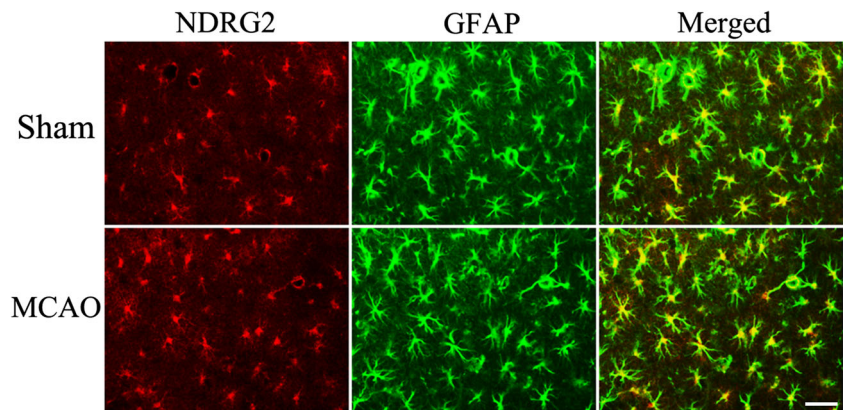


**Fig. 2** Expression of NDRG2 protein in different parts of the ischemic penumbra. **a** NDRG2 protein expression in cortex, striatum, and hippocampus of the ischemic penumbra at 24 h after reperfusion and in the sham-operated group. **b** The relative density of NDRG2 protein expression versus GAPDH protein expression was plotted. The data are expressed as the mean  $\pm$  S.D. *t* Test: \**p*<0.05 vs. the sham group

**Fig. 3** Immunofluorescence double-labeling of NDRG2 and GFAP. NDRG2 expression (*red*) and GFAP (*green*) in the sham-operated group and the 24 h after reperfusion group. The merged yellow images indicate co-localization of NDRG2 and GFAP. Bar = 20  $\mu$ m (color figure online)



### Up-regulation of NDRG2 Expression Inhibited the Proliferation of M1800 Cells

We successfully established cell lines in which NDRG2 expression was stably up- and down-regulated, as verified by Western blot analysis (Supplementary Fig. 2).

Cell proliferation was analyzed using an EdU incorporation assay and flow cytometric analysis. As shown in Fig. 6b, the percentage of EdU-positive cells was  $46.49 \pm 4.49$ ,  $48.09 \pm 4.80$ , and  $47.06 \pm 4.34$  % in the Con, KD-NC, and OE-NC groups, respectively, and there were no significant differences between these three groups. Down-regulation of NDRG2 expression in the KD group induced a significant increase in the percentage of EdU-positive cells (to  $63.31 \pm 5.09$  %) compared with that in the KD-NC group ( $*p < 0.05$ ). However, in the OE group, the percentage of EdU-positive cells significantly decreased (to  $33.31 \pm 4.95$  %) compared with that in the OE-NC group ( $\#p < 0.05$ ).

The flow cytometry results were consistent with those of the EdU incorporation assay. As shown in Fig. 7b,  $45.73 \pm 2.84$ ,  $45.98 \pm 3.81$ , and  $46.47 \pm 4.01$  % of cells were in S phase in the Con, KD-NC, and OE-NC groups, respectively, and  $52.37 \pm 3.51$ ,  $54.05 \pm 2.15$ , and  $52.81 \pm 2.90$  % of cells

were in either S + G2 phase. There were no significant differences between these three groups. In the KD group, down-regulation of NDRG2 expression induced a significant increase in the percentage of cells that were in S phase and that were in either S + G2 phase, to  $55.36 \pm 1.99$  and  $62.06 \pm 3.57$  %, respectively, compared with those in the KD-NC group ( $*p < 0.05$ ). However, in the OE group, the percentage of cells that were in S phase and that were in either S + G2 phase was significantly decreased, to  $36.42 \pm 2.94$  and  $43.09 \pm 2.55$  %, respectively, compared with those in the OE-NC group ( $\#p < 0.05$ ).

### Temporal Expression of NDRG2 in M1800 Cells Exposed to OGD-R

RT-PCR and Western blot were performed to evaluate the changes in NDRG2 expression that occurred in the astrocyte lines after OGD exposure. NDRG2 expression was significantly up-regulated in a time-dependent manner following OGD. Compared with the expression in the Con group, in the OGD group, both NDRG2 mRNA (Fig. 8a) and protein (Fig. 8b) expression began to increase 2 h after OGD and peaked at 24 h after OGD ( $*p < 0.05$ ; Fig. 8c).

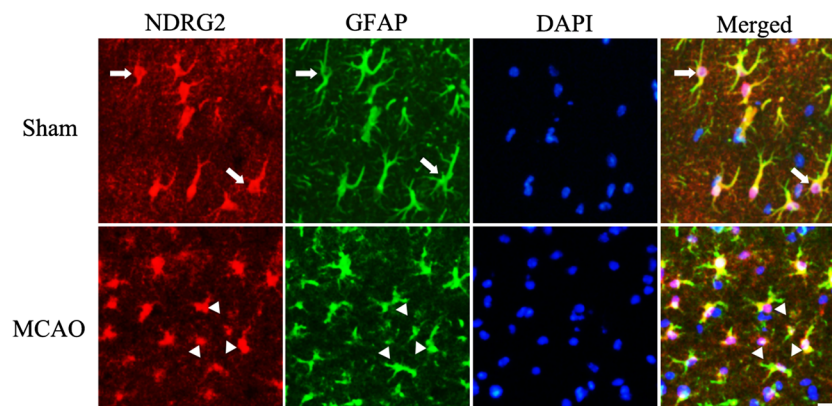
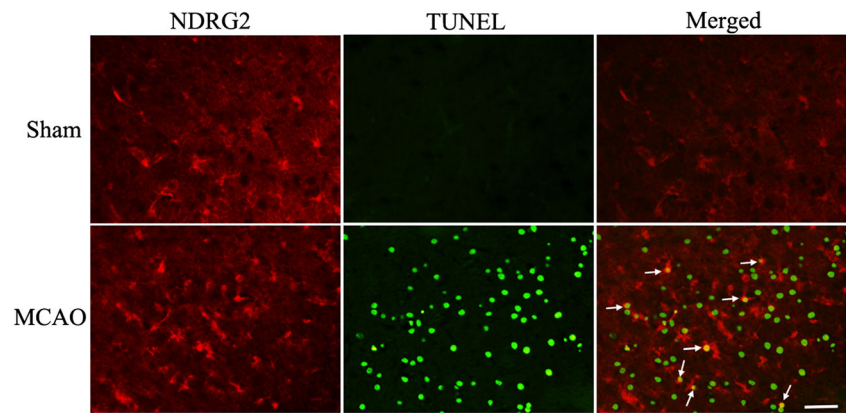


**Fig. 4** Cellular localization of NDRG2 in astrocytes by immunofluorescent labeling. In the sham-operated group, as *white arrows* show, NDRG2 (*red*) was expressed in the cytoplasm of astrocytes (*green*). In the ischemia-reperfusion group, as *white triangles* show, NDRG2 (*red*) was mainly located

in nucleus (*blue*) and weak in cytoplasm. DAPI (*blue*) was used to stain nucleus. The merged *purple images* indicate co-localization of NDRG2, GFAP, and DAPI. Bars = 20  $\mu$ m (color figure online)

**Fig. 5** Immunofluorescence TUNEL and NDRG2 staining. TUNEL (green) and NDRG2 (red) staining in the sham-operated group (sham group) and in the 24 h after reperfusion group (MCAO group). The merged yellow images indicate co-localization of NDRG2 and TUNEL (white arrowheads). Bar = 20  $\mu$ m (color figure online)



### In M1800 Cells, NDRG2 Was Translocated from the Cytoplasm to the Nucleus After OGD-R

As shown in Fig. 9a, in normal M1800 cells, NDRG2 was mainly co-localized with GFAP and there was little overlap with DAPI, indicating that the expression of NDRG2 was confined to the cytoplasm under normal conditions. However, the NDRG2 signal was markedly enhanced in the nuclei at 24 h after OGD exposure. The shift in NDRG2 expression indicated that NDRG2 was translocated from the cytoplasm to the nucleus, which was probably induced by the stress of OGD.

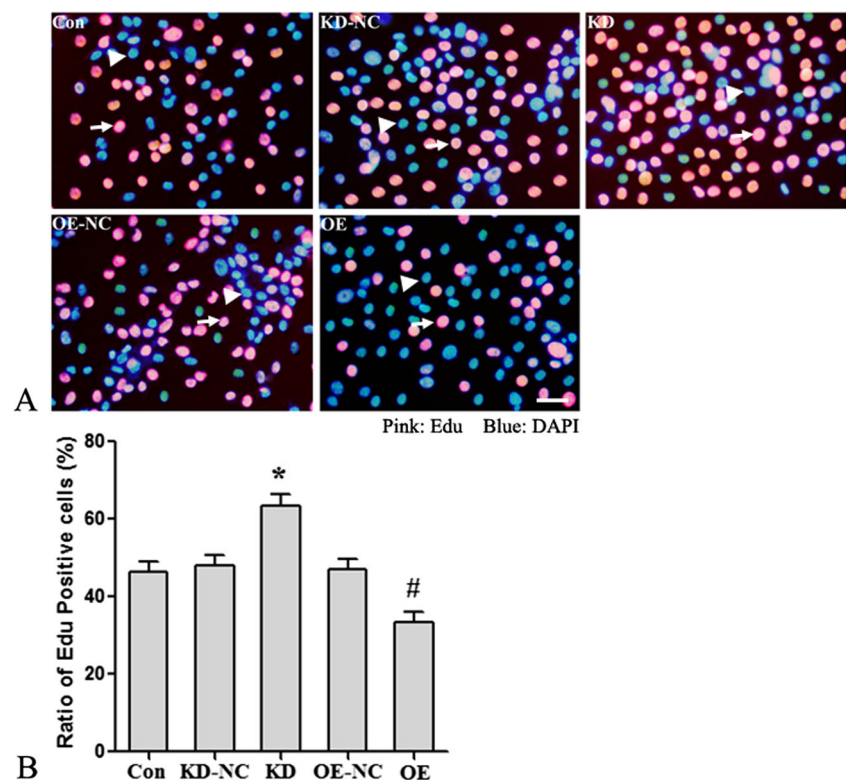
To further demonstrate the nuclear translocation of NDRG2 upon OGD exposure, a cell fraction assay was performed. As shown in Fig. 9b, under normal

conditions (sham group), NDRG2 was expressed mainly in the cytoplasm and could hardly be detected in the nuclei. After the cells were exposed to OGD, NDRG2 expression in both the nucleus and cytoplasm was sharply increased (OGD group).

### NDRG2 Promoted the Apoptosis of M1800 Cells Exposed to OGD-R

Flow cytometric analysis was used to assess the effect of NDRG2 on apoptosis after the cells were exposed to OGD-R (Fig. 10). In the Con, KD-NC, and OE-NC groups, the total apoptotic index was  $16.10 \pm 1.77$ ,  $19.70 \pm 2.55$ , and  $19.70 \pm 2.62$  %, respectively. There were no significant differences between these three

**Fig. 6** The effects of NDRG2 expression on the proliferation of cultured M1800 cells, as assessed by an EdU incorporation assay. **a** Triangles indicate DAPI-labeled nuclei (blue), and arrows indicate replicating DNA, as revealed by EdU incorporation (pink). **b** The data are expressed as the mean  $\pm$  S.D. *t* Test: \* $p < 0.05$  vs. the KD-NC group; # $p < 0.05$  vs. the OE-NC group (color figure online)



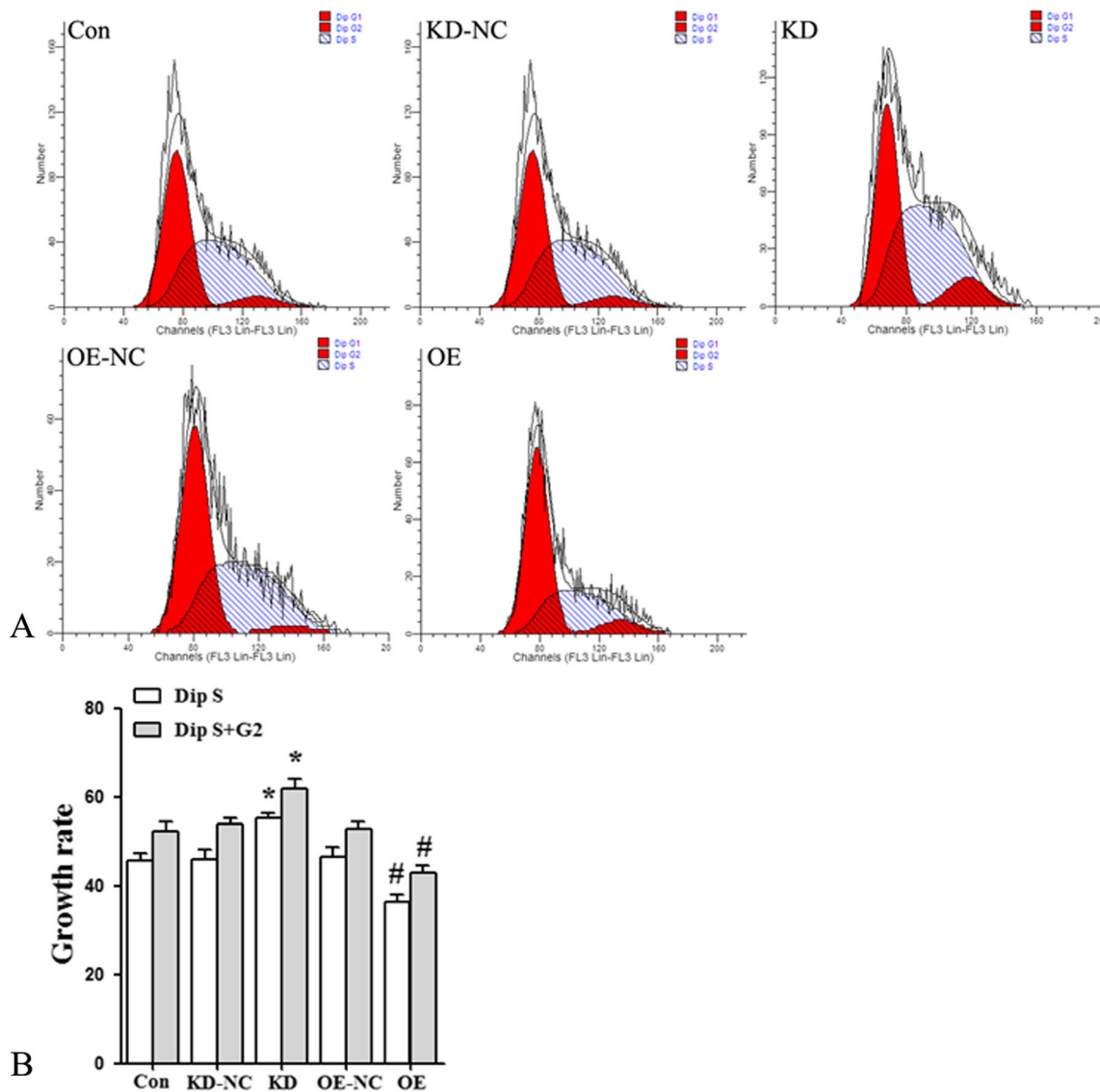


**Fig. 7** The effects of NDRG2 expression on the proliferation of cultured M1800 cells, as assessed by flow cytometric analysis. The first *red peak*, the *arc-shaped hatched portion* in the middle, and the second *red peak*

represent the G1, S, and G2 phases of the cell cycle, respectively. **b** The data are expressed as the mean  $\pm$  S.D. *t* Test: \* $p < 0.05$  vs. the KD-NC group; # $p < 0.05$  vs. the OE-NC group

groups. Down-regulation of NDRG2 expression (KD group) attenuated OGD-R-induced cell apoptosis to  $9.73 \pm 2.54$  % (\*\* $p < 0.01$  vs. the KD-NC group). Conversely, over-expression of NDRG2 (OE group) increased OGD-R-induced apoptosis to  $31.83 \pm 4.92$  % (# $p < 0.05$  vs. the OE-NC group).

As shown in Fig. 11, the M1800 cells exhibited stronger TUNEL-positive staining after OGD exposure, indicating that OGD induced cell apoptosis. Furthermore, the NDRG2 staining was co-localized with the TUNEL staining. However, down-regulation of NDRG2 expression (KD group) alleviated the OGD-induced TUNEL-positive staining, and over-expression of NDRG2 increased the OGD-induced TUNEL-positive staining.

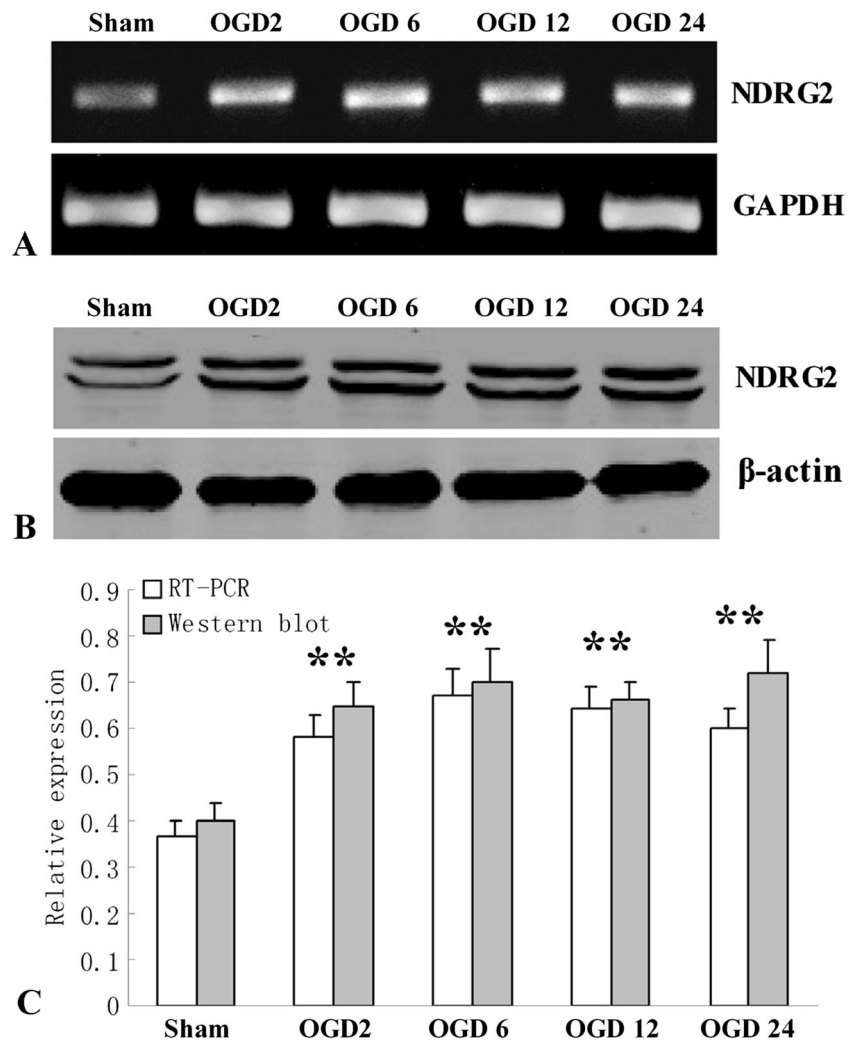
### NDRG2 Increased ROS Levels and Cleaved Caspase-3 Expression in M1800 Cells Exposed to OGD-R

As shown in Fig. 12, compared with those of the cells in the KD-NC group, the ROS levels in the cells in the KD group were significantly reduced after the cells were exposed to OGD-R (\* $p < 0.05$ ), and over-expression of NDRG2 (OE group) significantly increased ROS levels (# $p < 0.05$  vs. the OE-NC group). No significant differences were observed between the Con, KD-NC, and OE-NC groups.

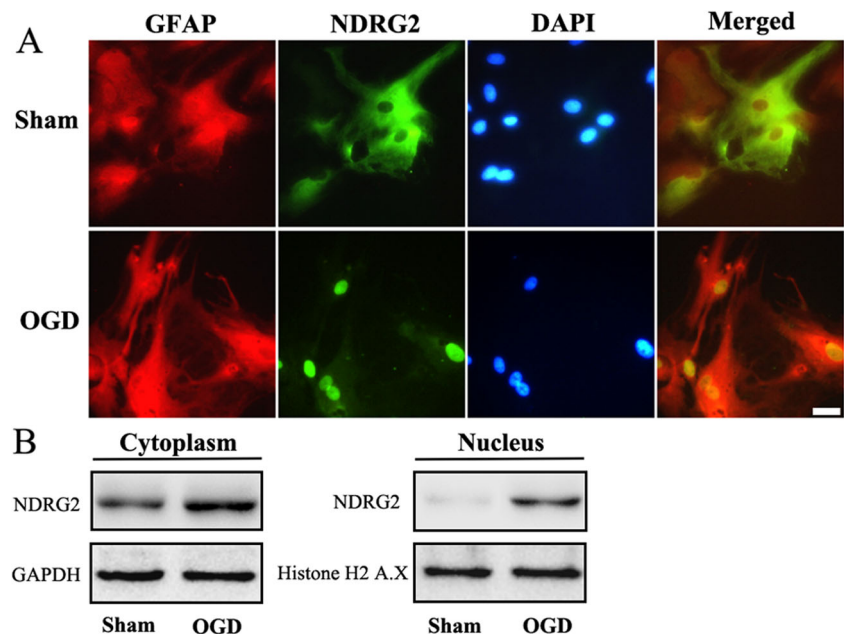
The results of the Western blot analysis of the protein expression of cleaved Caspase-3 (Fig. 13), which is a pro-apoptosis protein, show that compared with those of the cells in the KD-NC group, the expression levels of cleaved Caspase-3 protein in the cells in the KD group were



**Fig. 8** Temporal expression of NDRG2 in astrocyte cell lines exposed to OGD. **a** NDRG2 mRNA levels and **b** protein expression in the astrocyte cell lines at 2, 6, 12, and 24 h after OGD and in the sham-operated group. **c** The relative density of NDRG2 protein expression versus  $\beta$ -actin protein expression was plotted. The data are expressed as the mean  $\pm$  S.D. *t* Test:  $*p < 0.05$  vs. the sham group



**Fig. 9** NDRG2 nuclear translocation after OGD exposure. **a** Immunofluorescence double-labeling for NDRG2 (red) and DAPI (blue) showing the localization of NDRG2 in normal conditions and after OGD-R. Bar = 10  $\mu$ m. **b** NDRG2 expression in the nuclei and cytoplasmic fraction was measured using Western blotting. In normal cells, NDRG2 could hardly be detected in the nuclei. At 24 h after OGD exposure, NDRG2 expression was sharply increased in both the nucleus and cytoplasm (color figure online)



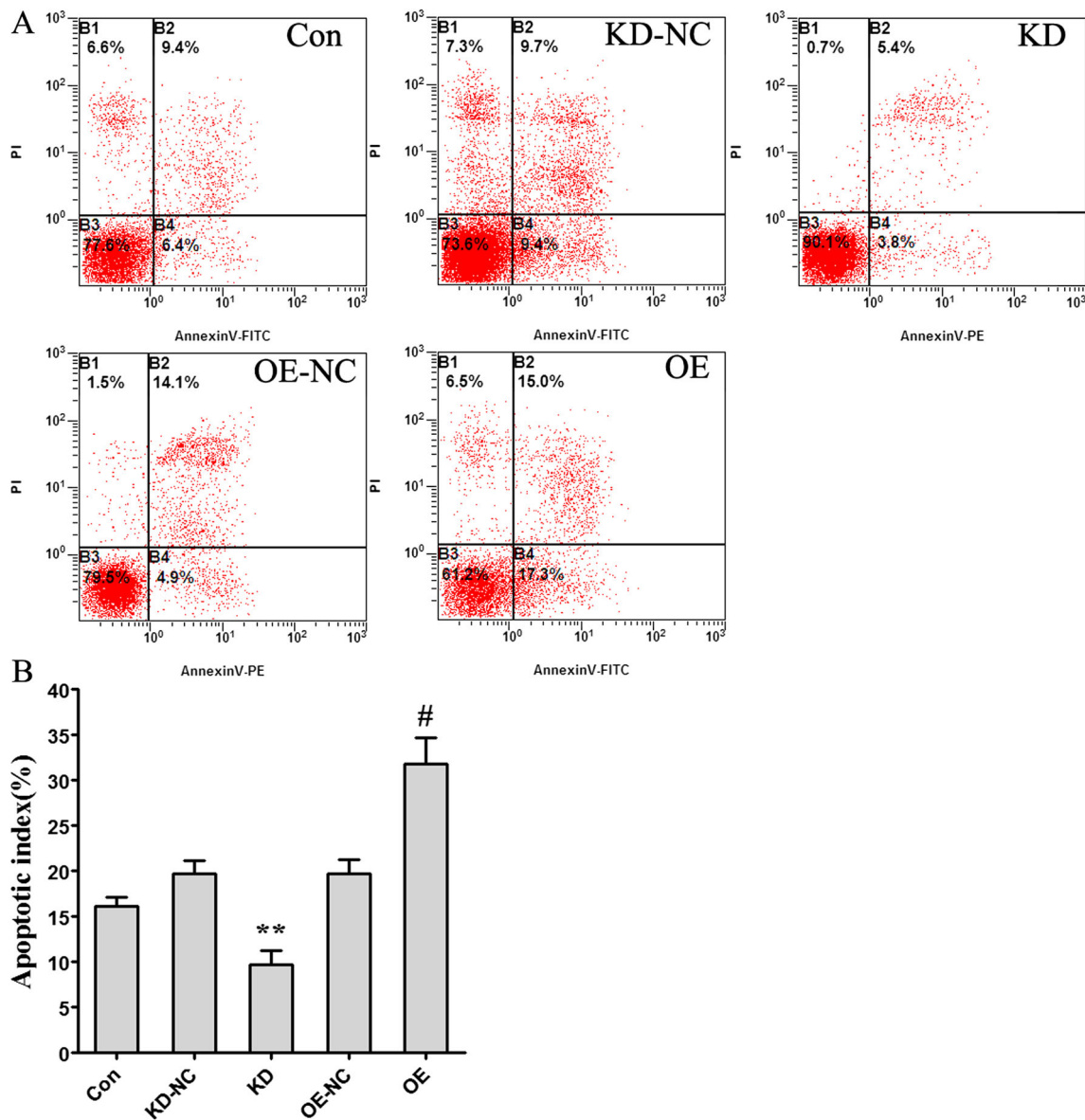


**Fig. 10** Effect of NDRG2 expression on OGD-R-induced cell apoptosis, as detected by flow cytometric analysis. **a** Representative photographs showing M1800 cell apoptosis induced by OGD-R in the various groups.

**b** The data are shown as the mean  $\pm$  S.D.; \*\* $p < 0.01$  vs. the KD-NC group; # $p < 0.05$  vs. the OE-NC group

significantly reduced after the cells were exposed to OGD-R ( $*p < 0.05$ ), and over-expression of NDRG2 (OE group) significantly increased cleaved Caspase-3 protein expression (# $p < 0.05$  vs. the OE-NC group). No significant differences were observed between the Con, KD-NC, and OE-NC groups.

## Discussion

Although many clinical trials of stroke patients have been completed, none of the evaluated therapeutics were shown to be protective, except thrombolytics [1, 18]. Importantly, the majority of the failed trials only targeted neuron-specific injury mechanisms [19]. A

large body of work has shown that astrocytes play key roles in both normal and pathological CNS functioning, and astrocytes are now thought to be important potential targets for stroke treatment [6]. Previous studies show that ischemia–hypoxia-induced astrocyte apoptosis, which seriously impairs astrocyte normal functions, contributes largely to neuronal injury [7]. The ischemic penumbra is the target for therapeutic interventions because salvage of this tissue is associated with neurological improvement and recovery [20]. Therefore, experimental approaches that reduce astrocyte apoptosis and enhance the function and survival of astrocytes in the ischemic penumbra may serve as a novel strategy against stroke.

**Fig. 11** Effect of NDRG2 expression on cell apoptosis, as demonstrated by TUNEL staining. Immunofluorescence double-labeling for NDRG2 (red) and TUNEL (green) was used to assess M1800 cell apoptosis 24 h after OGD. Bar = 10  $\mu$ m (color figure online)

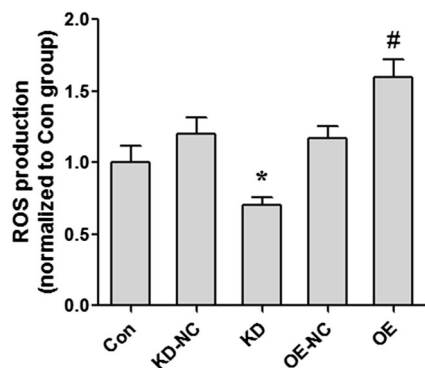
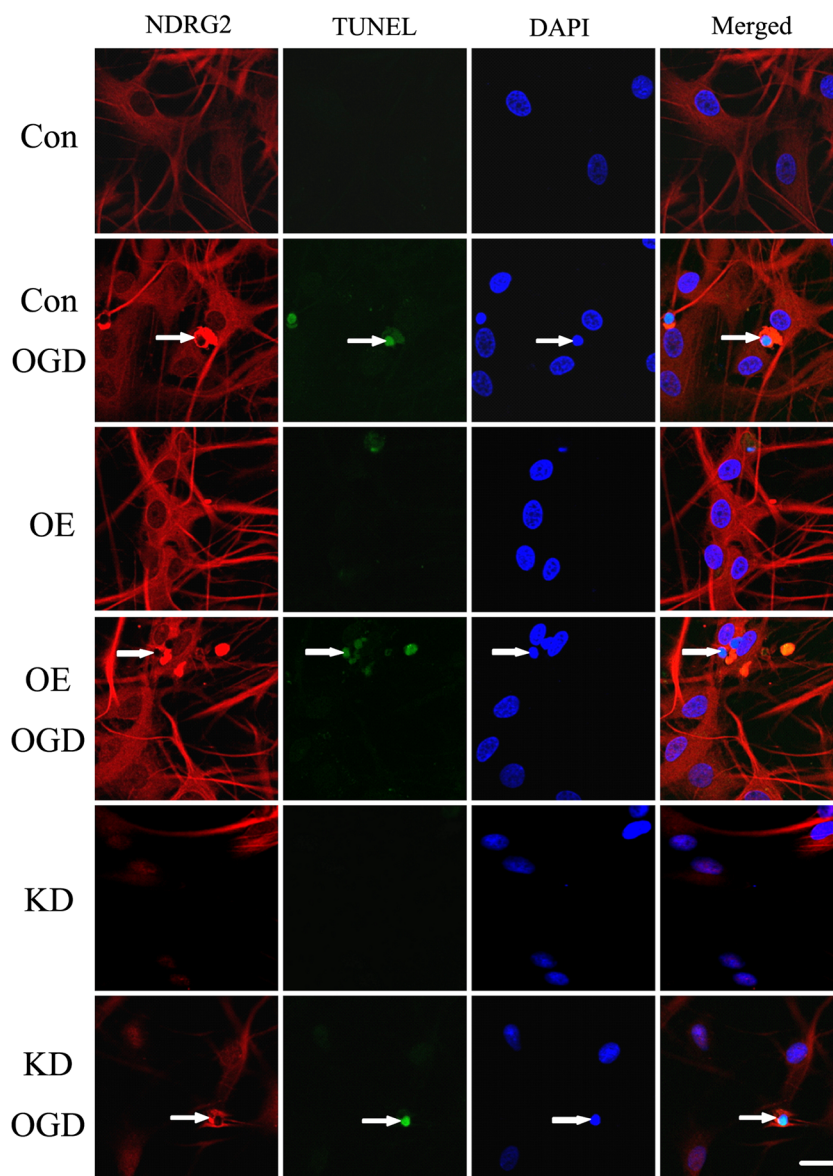


**Fig. 12** Effect of NDRG2 expression on ROS production in cells exposed to OGD-R. The data are shown as the mean  $\pm$  S.D.; \* $p$  < 0.05 vs. the KD-NC group; # $p$  < 0.05 vs. the OE-NC group

NDRG2 was first identified in 2001 [8], and our previous studies showed that NDRG2 is specifically expressed in CNS astrocytes [10, 21]. Several studies have demonstrated that NDRG2 is involved in AD [12], antidepressant treatments [13, 22], social stress [14], and frontotemporal lobar degeneration [15], demonstrating its role in pathological processes in the CNS. However, the role of NDRG2 in ischemic stroke has rarely been explored.

In the present study, we found that in the ischemic penumbra of mice, NDRG2 mRNA and protein expression was significantly increased at 6 h after reperfusion and peaked at 24 h. In *in vitro* experiments, we found that NDRG2 expression was significantly increased at 2 h after reperfusion and peaked at 24 h in M1800 cells. In a previous study [16], we found that in the ischemic penumbra of rats, NDRG2 expression was

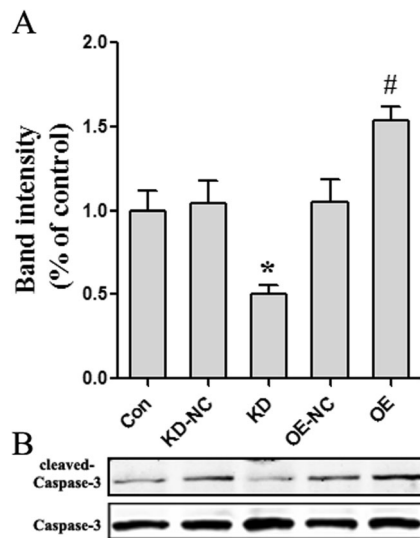


**Fig. 13** Effect of NDRG2 expression on cleaved Caspase-3 protein expression in cells exposed to OGD-R. **a** The data are shown as the mean  $\pm$  S.D.; \* $p < 0.05$  vs. the KD-NC group; # $p < 0.05$  vs. the OE-NC group. **b** Representative photographs showing cleaved Caspase-3 protein expression in the various groups

increased at 4 h after reperfusion and peaked at 24 h but then was decreased at 72 h. The difference may be due to the duration of the MCAO surgery as well as species differences between rats and mice. In addition, we found that in the cortex and striatum of the ischemic penumbra, which are more sensitive than the hippocampus to MCAO injury, NDRG2 protein expression significantly increased at 24 h after reperfusion. These results indicate that NDRG2 plays an important role in the pathogenesis of cerebral ischemia.

In the current study, we found that both in the ischemia and in M1800 cells, some NDRG2 signals were translocated from the cytoplasm to the nucleus after I/R or OGD-R. Nuclear translocation is a key step in cell signal transduction that frequently activates the transcription of genes involved in cellular differentiation and apoptosis. Based on the results described above, we hypothesized that NDRG2 may activate its downstream targets to regulate cell apoptosis following OGD-R. The activation of certain transcription factors leads to the translocation of molecules from the cytoplasm to the nucleus. However, the mechanisms that underlie NDRG2 nuclear translocation remain unclear. Previous studies found that residues 101–178 of NDRG2 or the  $\alpha 6$  helix of hNDRG2 might contribute to its translocation [23, 24]. Regardless, NDRG2 nuclear translocation indicates that NDRG2 plays an important role in cell signal transduction following OGD-R.

Ischemic injury peaked at 24 h after I/R in both the in vivo and in vitro experiments, suggesting that NDRG2 may contribute to cell damage in the ischemic penumbra. NDRG2 is very similar to NDRG1, which has been linked to apoptosis and may be an apoptosis-inducible factor [22]. Thus, we

investigated the relationship between NDRG2 expression and cell apoptosis in the ischemic penumbra following I/R and in M1800 cells exposed to OGD-R. Our results showed that as the number of NDRG2-positive cells increased in the ischemic penumbra and following OGD-R, the number of TUNEL-positive cells also increased. Importantly, we also found that NDRG2 was co-localized with the TUNEL-positive cells. These results demonstrated that NDRG2 was associated with the cell apoptosis induced by ischemia–hypoxia injury. To further explore the relationship between NDRG2 and cell apoptosis, we first constructed two stable astrocytic cell lines in which NDRG2 expression was significantly up- or down-regulated using a lentivirus. We found that NDRG2 over-expression significantly increased apoptotic cell numbers after OGD-R, whereas silencing NDRG2 expression had the opposite effect, which indicates that NDRG2 expression induced astrocyte apoptosis after ischemia–hypoxia injury. And ischemia–hypoxia could cause oxidative stress, which produces a lot of ROS and triggers the process of cell apoptosis [25]. Thus, we detected the effect of NDRG2 on astrocyte ROS production and found that NDRG2 over-expression significantly increased ROS production and cleaved Caspase-3 protein expression after OGD-R, whereas silencing NDRG2 expression had the opposite effect. These results indicate that NDRG2 expression promote astrocyte apoptosis by increasing ROS production. However, the underlying mechanism remains unclear and warrants further study.

Besides oxidative stress, there may be some other signal pathways involved in NDRG2-induced astrocyte apoptosis. Liu et al. [26] showed that NDRG2 is involved in p53-mediated apoptosis, and p53 also acts as a master regulator of cell death by inducing apoptosis [27]. A previous study reported that NDRG2 is a novel target of hypoxia-inducible factor-1 (HIF-1), which is necessary for hypoxia-induced apoptosis in A549 cells [23]. HIF-1 also plays an important role in stroke by regulating genes such as erythropoietin and VEGF [28]. Thus, it is possible that NDRG2 acts as p53 or HIF-1 target gene to regulate ischemia-induced apoptosis.

After ischemia, astrocytes support neurons by providing antioxidant protection [29], substrates for neuronal metabolism [30], and glutamate clearance REF; accordingly, impaired astrocyte function can amplify neuronal death [31]. In previous studies, we found that sevoflurane and electroacupuncture pre-conditioning inhibited NDRG2 up-regulation and nuclear translocation in astrocytes, resulting in increased cerebral ischemic tolerance by inhibiting astrocyte apoptosis [32, 33]. A recent study found attenuated neuronal death in *ndrg2* knock-out (*ndrg2*<sup>-/-</sup>) mice after cortical stab injury [34]. Therefore, the use of NDRG2 as a molecular target for the reduction of astrocyte apoptosis may become a new therapeutic strategy for ischemic stroke.

In addition, because NDRG2 has been shown to be a pro-differentiative and anti-proliferative gene in previous cancer

research and is now considered a tumor suppressor [24], we examined the effect of NDRG2 on cell proliferation and found that NDRG2 over-expression significantly inhibited the rate of cell proliferation, consistent with studies of human glioblastomas infected with *Ndr2* cDNA [35]. Takeichi et al. [36] found that in cultured astrocytes, silencing of the *Ndr2* gene significantly enhanced the numbers of cells that incorporated 5-bromo-2'-deoxy-uridine (BrdU) that were positive for proliferating cell nuclear antigen (PCNA) by enhancing the transcription of cell cycle molecules, such as CyclinB1 and CyclinE. However, the particular mechanism underlying the effect of NDRG2 on cell growth must be further defined.

This study had some limitations, and certain questions still remain. First, we selected only one time point (24 h after reperfusion) at which to evaluate the role of NDRG2 in the ischemic penumbra. This time point represents the acute phase of reperfusion, but the involvement of NDRG2 in the late phase of reperfusion (>72 h after reperfusion) remains unknown and warrants further study. Second, we did not explore the role of NDRG2 in astrocyte–neuron interactions, which might be an even more important mechanism. Hence, we plan to use *ndrg2*<sup>-/-</sup> mice to investigate the role of NDRG2 in ischemic stroke in future studies. Third, astrocytes exhibit many cellular responses to ischemic injury, including influencing material and energy metabolism [30], glutamate excitotoxicity [37], and so forth. However, whether the increase in NDRG2 expression is related to these astrocyte functions remains unknown, and this will be the focus of our future work.

In conclusion, the current study demonstrated that up-regulation of the astrocyte-specific protein NDRG2 in the ischemic penumbra and in astrocytes exposed to OGD-R is involved in astrocyte apoptosis and that inhibiting NDRG2 expression significantly reduced ROS production and astrocyte apoptosis following exposure to OGD-R. Although further investigations are needed to elucidate the detailed signaling cascades underlying the NDRG2 pathway, our findings provide potential targets for future clinical therapies for stroke.

**Acknowledgments** This study was supported by the Natural Science Foundation of China (81571279; 81371446; 81403451; 81370194), China Postdoctoral Science Foundation (2014M562560; 2015T81110), and Beijing Natural Science Foundation (7154242). We thank American Journal Experts (AJE) for assisting in the preparation of this manuscript.

**Compliance with Ethical Standards** All animal experimental procedures followed a protocol approved by the Ethics Committee for Animal Experimentation of the Fourth Military Medical University, China.

## References

- Marder VJ, Jahan R, Gruber T, Goyal A, Arora V (2010) Thrombolysis with plasmin: implications for stroke treatment. *Stroke* 41:S45–S49. doi:10.1161/STROKEAHA.110.595157
- Sofroniew MV, Vinters HV (2010) Astrocytes: biology and pathology. *Acta Neuropathol* 119:7–35. doi:10.1007/s00401-009-0619-8
- Iadecola C, Nedergaard M (2007) Glial regulation of the cerebral microvasculature. *Nat Neurosci* 10:1369–1376. doi:10.1038/nn2003
- Brown AM, Ransom BR (2007) Astrocyte glycogen and brain energy metabolism. *Glia* 55:1263–1271. doi:10.1002/glia.20557
- Perea G, Navarrete M, Araque A (2009) Tripartite synapses: astrocytes process and control synaptic information. *Trends Neurosci* 32:421–431. doi:10.1016/j.tins.2009.05.001
- Barreto G, White RE, Ouyang Y, Xu L, Giffard RG (2011) Astrocytes: targets for neuroprotection in stroke. *Cent Nerv Syst Agents Med Chem* 11:164–173. doi:10.2174/187152411796011303
- Takuma K, Baba A, Matsuda T (2004) Astrocyte apoptosis: implications for neuroprotection. *Prog Neurobiol* 72:111–127. doi:10.1016/j.pneurobio.2004.02.001
- Deng YC, Yao LB, Liu XP (2001) Exploring a new gene containing ACP like domain in human brain and expression of it in *E. coli*. *Prog Biochem Biophys* 28:72–76
- Boulkroun S, Fay M, Zennaro MC, Escoubet B, Jaisser F, Blot-Chaubaud M, Farman N, Courtois-Coutry N (2002) Characterization of rat NDRG2 (N-Myc downstream regulated gene 2), a novel early mineralocorticoid-specific induced gene. *J Biol Chem* 277:31506–31515. doi:10.1074/jbc.M200272200
- Ma YL, Qin P, Feng DY, Li Y, Zhang LX, Liu ZY, Yin AQ, Tang WH et al (2014) Estrogen regulates the expression of *Ndr2* in astrocytes. *Brain Res* 1569:1–8
- Flügge G, Araya-Callis C, Garea-Rodriguez E, Stadelmann-Nessler C, Fuchs E (2014) NDRG2 as a marker protein for brain astrocytes. *Cell Tissue Res* 357:31–41. doi:10.1007/s00441-014-1837-5
- Mitchelmore C, Büchmann-Møller S, Rask L, West MJ, Troncoso JC, Jensen NA (2004) NDRG2: a novel Alzheimer's disease associated protein. *Neurobiol Dis* 16:48–58. doi:10.1016/j.nbd.2004.01.003
- Takahashi K, Yamada M, Ohata H, Momose K, Higuchi T, Honda K, Yamada M (2005) Expression of *Ndr2* in the rat frontal cortex after antidepressant and electroconvulsive treatment. *Int J Neuropsychopharmacol* 8:381–389. doi:10.1017/S1461145705005134
- Araya-Callis C, Hiemke C, Abumaria N, Flugge G (2012) Chronic psychosocial stress and citalopram modulate the expression of the glial proteins GFAP and NDRG2 in the hippocampus. *Psychopharmacology (Berlin)* 224:209–222. doi:10.1007/s00213-012-2741-x
- Herskowitz JH, Seyfried NT, Duong DM, Xia Q, Rees HD, Gearing M, Peng J, Lah JJ et al (2010) Phosphoproteomic analysis reveals site-specific changes in GFAP and NDRG2 phosphorylation in frontotemporal lobar degeneration. *J Proteome Res* 9:6368–6379. doi:10.1021/pr100666c
- Li Y, Shen L, Cai L, Wang Q, Hou W, Wang F, Zeng Y, Zhao G et al (2011) Spatial-temporal expression of NDRG2 in rat brain after focal cerebral ischemia and reperfusion. *Brain Res* 1382:252–258. doi:10.1016/j.brainres.2011.01.023
- Yang Q, Yan W, Li X, Hou L, Dong H, Wang Q, Dong H, Wang S et al (2012) Activation of canonical notch signaling pathway is involved in the ischemic tolerance induced by sevoflurane preconditioning in mice. *Anesthesiology* 117:996–1005. doi:10.1097/ALN.0b013e31826cb469
- Blakeley JO, Llinas RH (2007) Thrombolytic therapy for acute ischemic stroke. *J Neurol Sci* 261:55–62. doi:10.1016/j.jns.2007.04.031
- Howells DW, Porritt MJ, Rewell SS, O'Collins V, Sena ES, van der Worp HB, Traystman RJ, Macleod MR (2010) Different strokes for different folks: the rich diversity of animal models of focal cerebral

- ischemia. *J Cereb Blood Flow Metab* 30:1412–1431. doi:10.1038/jcbfm.2010.66
20. Weinstein PR, Hong S, Sharp FR (2004) Molecular identification of the ischemic penumbra. *Stroke* 35(11 Suppl 1):2666–2670. doi:10.1161/01.STR.0000144052.10644.ed
  21. Hu XL, Liu XP, Deng YC, Lin SX, Wu L, Zhang J, Wang LF, Wang XB et al (2006) Expression analysis of the NDRG2 gene in mouse embryonic and adult tissues. *Cell Tissue Res* 325:67–76. doi:10.1007/s00441-005-0137-5
  22. Nichols NR (2003) Ndr2, a novel gene regulated by adrenal steroids and antidepressants, is highly expressed in astrocytes. *Ann N Y Acad Sci* 1007:349–356. doi:10.1196/annals.1286.034
  23. Wang L, Liu N, Yao L, Li F, Zhang J, Deng Y, Liu J, Ji S et al (2008) NDRG2 is a new HIF-1 target gene necessary for hypoxia-induced apoptosis in A549 cells. *Cell Physiol Biochem* 21:239–250. doi:10.1159/000113765
  24. Hwang J, Kim Y, Kang HB, Jaroszewski L, Deacon AM, Lee H, Choi WC, Kim KJ et al (2011) Crystal structure of the human N-Myc downstream-regulated gene 2 protein provides insight into its role as a tumor suppressor. *J Biol Chem* 286:12450–12460. doi:10.1074/jbc.M110.170803
  25. Hou CW, Lin YT, Chen YL, Wang YH, Chou JL, Ping LY, Jeng KC (2012) Neuroprotective effects of camosic acid on neuronal cells under ischemic and hypoxic stress. *Nutr Neurosci* 15:257–263. doi:10.1179/1476830512Y.0000000021
  26. Liu N, Wang L, Li X, Yang Q, Liu X, Zhang J, Zhang J, Wu Y et al (2008) N-Myc downstream-regulated gene 2 is involved in p53-mediated apoptosis. *Nucleic Acids Res* 36:5335–5349. doi:10.1093/nar/gkn504
  27. Schmitt CA, Fridman JS, Yang M, Baranov E, Hoffman RM, Lowe SW (2002) Dissecting p53 tumor suppressor functions in vivo. *Cancer Cell* 1:289–298. doi:10.1016/S1535-6108(02)00047-8
  28. Bernaudin M, Nedelec AS, Divoux D, MacKenzie ET, Petit E, Schumann-Bard P (2002) Normobaric hypoxia induces tolerance to focal permanent cerebral ischemia in association with an increased expression of hypoxia-inducible factor-1 and its target genes, erythropoietin and VEGF, in the adult mouse brain. *J Cereb Blood Flow Metab* 22:393–403. doi:10.1097/00004647-200204000-00003
  29. Dringen R, Hirrlinger J (2003) Glutathione pathways in the brain. *Biol Chem* 384:505–516. doi:10.1515/BC.2003.059
  30. Rossi DJ, Brady JD, Mohr C (2007) Astrocyte metabolism and signaling during brain ischemia. *Nat Neurosci* 10:1377–1386. doi:10.1038/nn2004
  31. Nedergaard M, Dirnagl U (2005) Role of glial cells in cerebral ischemia. *Glia* 50:281–286. doi:10.1002/glia.20205
  32. Wang F, Gao Z, Li X, Li Y, Li X, Zhong H, Xu N, Cao F et al (2013) NDRG2 is involved in anti-apoptosis induced by electroacupuncture pretreatment after focal cerebral ischemia in rats. *Neurol Res* 35:406–414. doi:10.1179/1743132813Y.0000000159
  33. Li X, Luo P, Wang F, Yang Q, Li Y, Zhao M, Wang S, Wang Q et al (2014) Inhibition of N-myc downstream-regulated gene-2 is involved in an astrocyte-specific neuroprotection induced by sevoflurane preconditioning. *Anesthesiology* 121:549–562. doi:10.1097/ALN.0000000000000314
  34. Takarada-Iemata M, Kezuka D, Takeichi T, Ikawa M, Hattori T, Kitao Y, Hori O (2014) Deletion of N-myc downstream-regulated gene 2 attenuates reactive astrogliosis and inflammatory response in a mouse model of cortical stab injury. *J Neurochem* 130:374–387. doi:10.1111/jnc.12729
  35. Deng Y, Yao L, Chau L, Ng SS, Peng Y, Liu X, Au WS, Wang J et al (2003) N-Myc downstream-regulated gene 2 (NDRG2) inhibits glioblastoma cell proliferation. *Int J Cancer* 106:342–347. doi:10.1002/ijc.11228
  36. Takeichi T, Takarada-Iemata M, Hashida K, Sudo H, Okuda T, Kokame K, Hatano T, Takanashi M et al (2011) The effect of Ndr2 expression on astroglial activation. *Neurochem Int* 59:21–27. doi:10.1016/j.neuint.2011.03.019
  37. Swanson RA, Ying W, Kauppinen TM (2004) Astrocyte influences on ischemic neuronal death. *Curr Mol Med* 4:193–205. doi:10.2174/1566524043479185